Journal of Sound and Vibration (1999) **219**(3), 483–502
Article No. jsvi.1998.1869, available online at http://www.idealibrary.com.on IDEAL

DYNAMIC STIFFNESS OF A RAILWAY OVERHEAD WIRE SYSTEM AND ITS EFFECT ON PANTOGRAPH–CATENARY SYSTEM DYNAMICS

T. X. Wu

Department of Mechanical Engineering, Shanghai Tiedao University, Shanghai 2000331, *People's Republic of China*

AND

M. J. Brennan

*Institute of Sound and Vibration Research, University of Southampton, Highfield, Southampton SO*17 1*BJ, England*

(*Received* 28 *April* 1998, *and in final form* 23 *July* 1998)

For an electrical railway overhead wire system there are two main factors which crucially affect the quality of current collection. One is the spatial stiffness variation of the overhead wire along each span and the other is the flexural wave motion in the wire. In this paper a periodically excited single-degree-of-freedom (SDOF) model of a combined pantograph–catenary system is introduced and its basic dynamic behaviour is discussed. To investigate the effect of wave propagation in the overhead wire on vibration of the pantograph the dynamic stiffness of the catenary is introduced into the model. The dynamic stiffness of the catenary is determined by representing the overhead wire system as an infinite periodically spring-supported string. The results show that the dynamic stiffness of the catenary varies with train speed and its effect on the performance of the pantograph–catenary system is discussed.

1. INTRODUCTION

High-speed electrical railway systems are competitive with airlines for relatively short journeys. However, at high-speeds one of the main problems for electric railways is the maintenance of smooth, continuous current collection. This task is accomplished by a pantograph mounted on the locomotive roof which is in contact with an overhead wire (catenary). Unfortunately, as operational train speeds increase, vibration of the pantograph and overhead wire also increases. This may lead to a zero contact force between the pantograph and the catenary, resulting in loss of contact, arcing and wear. A recent review paper discussing the state of the art of pantograph/catenary systems has been presented by Poetsch *et al*. [1].

0022–460X/99/030483 + 20 $30.00/0

The pantograph and the catenary together form a dynamically coupled vibrating system affecting each other through the contact force. The main source of vibration is the spatial stiffness variation of the catenary along the span [2]; in the middle of a span the stiffness of the catenary is minimum and near the support tower it is maximum. When the pantograph moves along the catenary, the stiffness variation produces a periodic excitation which leads to vibration of the pantograph and fluctuation of the contact force. In addition, as the pantograph head (panhead) moves along the catenary, it causes a flexural wave motion in the wire. This flexural wave propagation also affects the contact force and the motion of the pantograph.

The dynamic interaction of the pantograph and the catenary has been studied extensively. An approximate analytical formulation to determine the contact force has been presented by Ockendon and Taylor [3]. Vinayagalingam [4] studied the contact force variation and the panhead trajectory by using finite difference methods, and Wu [5] developed a finite element model of the pantograph–catenary system to study the current collection problem by numerical simulation. Wormley *et al*. [6] obtained the free vibration modes of the overhead wire system and the contact force by using the Rayleigh–Ritz and modal analysis methods, respectively. Yagi *et al*. [7] investigated the dynamic response of the pantograph–catenary system to the lateral movement of the overhead wire due to its zigzag layout.

Although different aspects of the pantograph–catenary system's dynamics have been studied, a comprehensive analytical model of this coupled system has not been reported so far. Some researchers have tried to obtain a better understanding of the system's dynamic behaviour by using a relatively simple model. A periodically excited single-degree-of-freedom (SDOF) model representing the basic dynamics of the combined pantograph–catenary system has been proposed by Wu and Brennan [8]. This model is simple and retains most of the basic dynamic properties of the system. However, the catenary was modelled as a massless spatially fluctuating static stiffness, and hence wave propagation in the catenary was neglected. Manabe [9] used wave analysis to study the response of a catenary with discrete support springs to a travelling constant load which represents a pantograph. It is clear from this work that the dynamic displacements of a catenary subjected to a moving load will vary with the speed of the load and thus the dynamic stiffness of the catenary should be considered in a comprehensive study of pantograph–catenary dynamics. A comprehensive theory of the effect of moving loads on structures can be found in Frýba's book [10].

The aim of this paper is to obtain a better understanding of the pantograph–catenary system dynamics. Although complicated models and numerical methods are useful to obtain some specific solutions, a relatively simple analytical model is more appropriate to gain the physical insight into the pantograph–catenary system. Essentially, Wu and Brennan's model [8] is improved upon by introducing the dynamic stiffness of the catenary and the effects of this on the performance of the pantograph–catenary system are investigated. The paper is organised in six sections. Following the introduction, the periodically excited SDOF model of the pantograph–catenary system is presented in

section 2. In section 3 the overhead wire system is simplified to an infinite periodically spring-supported string, and its dynamic response to a moving load is investigated using a semi-analytical method based on Floquet's theory. In section 4 a more precise description of the pantograph–catenary system's dynamic properties is achieved by using the dynamic stiffness of the catenary. Before concluding the paper two numerical examples are presented in section 5, one for a mid-speed and one for a high-speed railway.

Because the target of this paper is to study the interaction between the pantograph and the catenary, some factors such as initial sag of the catenary, fundamental excitation of the locomotive roof and aerodynamic force to the pantograph are not included in the analysis.

2. INTERACTION OF THE PANTOGRAPH AND THE CATENARY

In this section Wu and Brennan's model for the pantograph–catenary system dynamics [8] is briefly reviewed. This is included in this paper to introduce the concept of a combined pantograph–catenary system and to show the fundamental excitation mechanism.

2.1. STATIC STIFFNESS FLUCTUATION OF THE CATENARY

A picture of a real pantograph–catenary system is shown in Figure 1 and schematic diagrams of two types of catenary are shown in Figure 2. The compound catenary is used for high-speed trains (usually above about 200 km/h) and the simple catenary for mid-speed trains (usually below about 150 km/h). Because the compound catenary is more complicated, it is more expensive than the simple catenary. The Finite Element Method (FEM) can be used to calculate the static stiffness of the catenary [2] and Figure 3 shows the static stiffness variation in a single span for the two types of catenary. The tensions used in the calculations

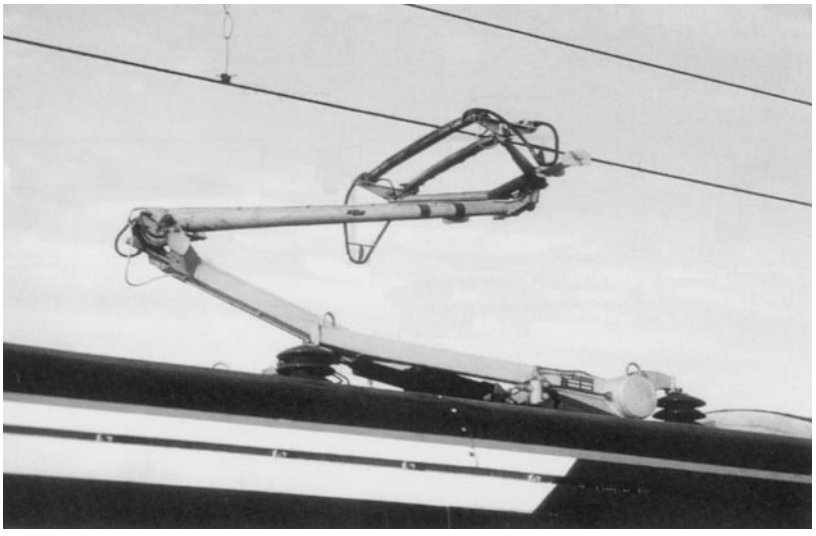

Figure 1. A pantograph–catenary system in operation.

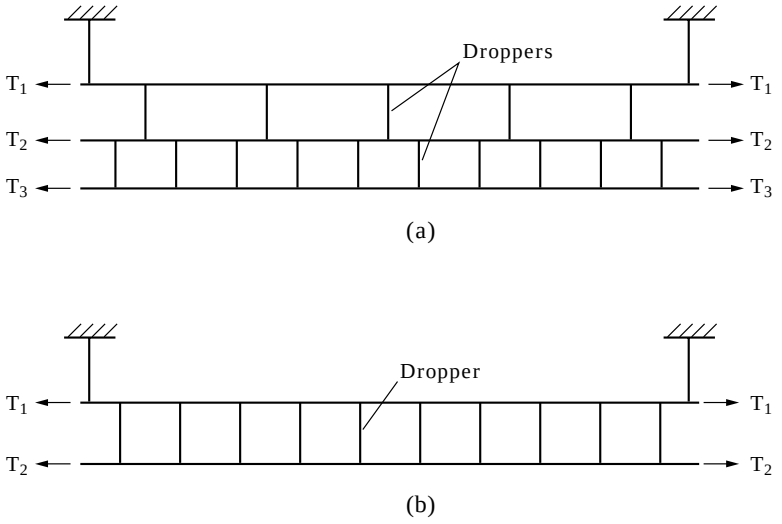

Figure 2. Two types of catenary system: (a) compound catenary; (b) simple catenary.

are typical of practical installations and are given in reference [11]. It can be seen that the stiffness fluctuation of the compound catenary is far smaller than that of the simple catenary and, as will be shown later, this enables a higher operational train speed.

2.2. MODELLING OF THE PANTOGRAPH–CATENARY SYSTEM

The modelling procedure is shown schematically in Figure 4. In Figure 4(a) the upper mass M_1 represents the panhead, and the lower mass M_2 represents the equivalent inertia of the pantograph frame. K_1 and C_1 represent the stiffness and the damping between the head and the frame, respectively, and C_2 represents the damping between the frame and the base. F_L is the uplift force which is produced by air pressure or spring loading and may be regarded as constant. If the mass of the catenary is neglected and K_1 is much greater than the stiffness of the catenary, then the model can be simplified to a SDOF model. This is shown in

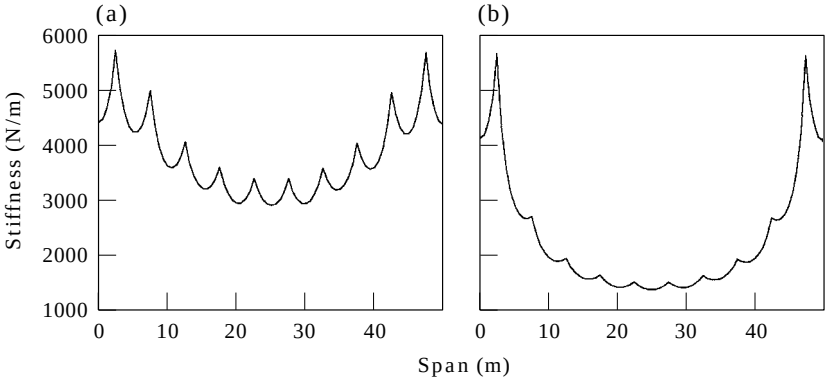

Figure 3. Static stiffness of contact wire in a span: (a) compound catenary $T_1 = 24{\cdot}5$ kN, $T_2 = T_3 = 14{\cdot}7$ kN; (b) simple catenary $T_1 = T_2 = 9{\cdot}8$ kN.

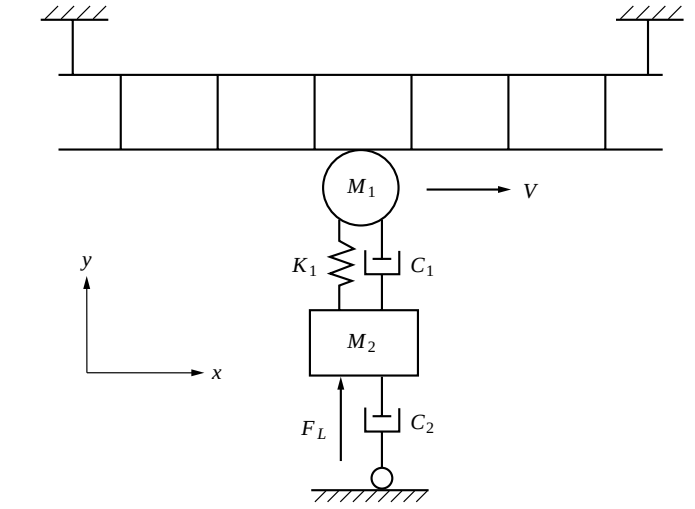

(a)

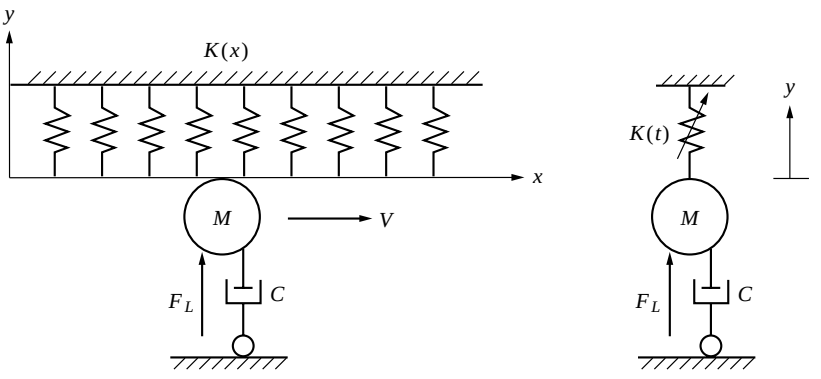

(b)

Figure 4. Model of the pantograph–catenary system.

Figure 4(b) where the time-varying stiffness $K(t)$ represents the catenary, and $M = M_1 + M_2$ represents the dynamic mass of the whole pantograph. The equation of motion describing the SDOF model in Figure 4(b) is

$$M\ddot{y} + C\dot{y} + K(t)y = F_L. \tag{1}$$

If we omit the stiffness variation between the vertical droppers and consider a train travelling with constant speed V, then $K(t)$ can be written as

$$K(t) = K_0\left(1 - \alpha \cos \frac{2\pi V}{L} t\right), \tag{2a}$$

where L is the length of one span and

$$K_0 = \frac{K_{max} + K_{min}}{2}, \qquad \alpha = \frac{K_{max} - K_{min}}{K_{max} + K_{min}}, \tag{2b, c}$$

where K_{max} and K_{min} are the largest and smallest stiffness in a span, respectively. K_0 and α can be regarded as the average stiffness and the stiffness variation coefficient, respectively. If we set $\omega_n^2 = K_0/M$ and $\omega = 2\pi V/L$, where ω_n is defined as the nominal natural frequency of the pantograph–catenary system and ω is the frequency of the stiffness variation which is related to train speed and the length of a span, then equation (1) can be written as

$$\ddot{y} + \frac{C}{M}\dot{y} + \omega_n^2(1 + \alpha \cos \omega t)y = \frac{F_L}{M}. \tag{3}$$

This equation can be non-dimensionalised by letting $\tau = \omega_n t$ to give

$$\frac{\mathrm{d}^2 y}{\mathrm{d}\tau^2} + 2\zeta \frac{\mathrm{d}y}{\mathrm{d}\tau} + (1 + \alpha \cos t\tau)y = f, \tag{4}$$

where

$$2\zeta = \frac{C}{\omega_n M}, \qquad r = \frac{\omega}{\omega_n} = \frac{2\pi V}{\omega_n L}, \qquad f = \frac{F_L}{K_0}.$$

Equation (4) can be recognised as the forced, damped Mathieu equation [12]. Two parameters determined the dynamic behaviour of the pantograph–catenary system. They are α which represents the stiffness variation of the catenary, and r which is related to the speed of the train, the span length and the nominal natural frequency of the system. By examining equation (4) we can determine the behaviour of the pantograph–catenary system.

2.3. STABILITY OF THE SYSTEM

Since equation (4) represents a parametrically excited system, its stability boundaries which are dependent upon α, ζ and r should be determined first. According to the data in reference [11], for a compound catenary the stiffness variation coefficient α is about 0·3 and for a simple catenary α it is about 0·6. Current operational train speeds are below 500 km/h, so the coefficient r is less than 1·5. The stability boundaries of the pantograph–catenary system described by equation (4) can be obtained by using Floquet's theory [12] and the results are shown in Figure 5. Three unstable areas occur in regions around $r = 2/3$, 1 and 2, and they are dependent upon damping. As a realistic damping coefficient for the pantograph is generally greater than 0·02, a practical pantograph–catenary system will probably not suffer from instabilities. Therefore, the loss of contact between the pantograph and the catenary at higher speeds will be caused by normal vibration of the pantograph rather than unbounded or unstable vibration.

2.4. DYNAMIC DISPLACEMENT AND CONTACT FORCE

An approximate analytical solution to equation (4) can be obtained by using the perturbation method. It has been shown that the transient response vanishes with increasing time [13], thus it is only necessary here to study the steady-state

response. A fourth order approximate steady-state response to a constant uplift force is given as follows [8]:

$$y = y_0 + \alpha y_1 + \alpha^2 y_2 + \alpha^3 y_3$$

$$= f\left\{1 - \frac{\alpha}{\sqrt{R_1}}\left\{\cos(r\tau - \varphi_1) - \frac{\alpha}{2}\left[\cos\varphi_1 + \frac{1}{\sqrt{R_2}}\cos(2r\tau - \varphi_1 - \varphi_2)\right]\right.\right.$$

$$-\frac{\alpha^2}{4}\left[\frac{2\cos\varphi_1}{\sqrt{R_1}}\cos(r\tau - \varphi_1) + \frac{1}{\sqrt{R_2}}\left[\frac{1}{\sqrt{R_1}}\cos(r\tau - 2\varphi_1 - \varphi_2)\right.\right.$$

$$\left.\left.\left.\left.+\frac{1}{\sqrt{R_3}}\cos(3r\tau - \varphi_1 - \varphi_2 - \varphi_3)\right]\right]\right\}\right\}, \tag{5}$$

where

$$R_1 = (1 - r^2)^2 + (2\zeta r)^2, \qquad \varphi_1 = \tan^{-1}\frac{2\zeta r}{1 - r^2}, \tag{6a}$$

$$R_2 = (1 - 4r^2)^2 + (4\zeta r)^2, \qquad \varphi_2 = \tan^{-1}\frac{4\zeta r}{1 - 4r^2}, \tag{6b}$$

$$R_3 = (1 - 9r^2)^2 + (6\zeta r)^2, \qquad \varphi_3 = \tan^{-1}\frac{6\zeta r}{1 - 9r^2}. \tag{6c}$$

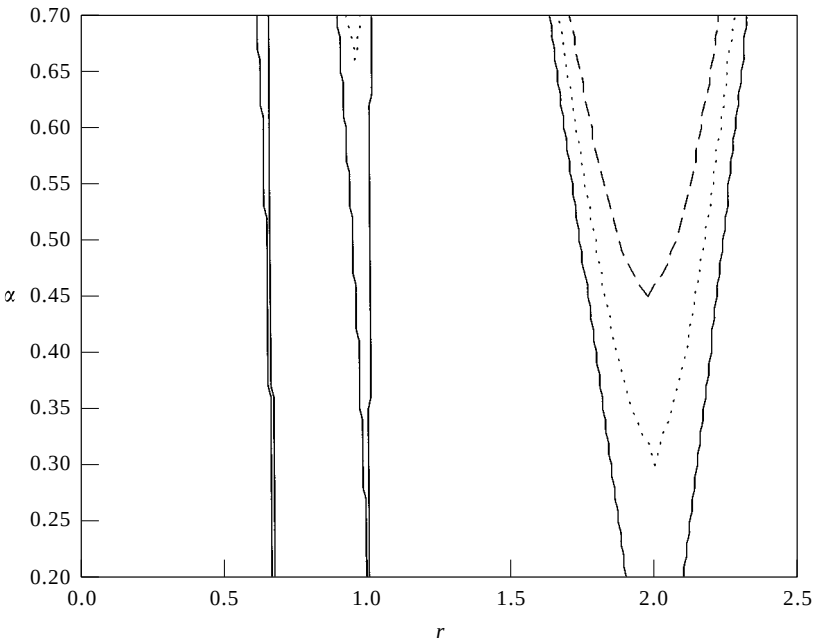

Figure 5. Stable and unstable regions of the pantograph–catenary system.——, $\zeta = 0$; · · · · · · · , $\zeta = 0{\cdot}01$; – – –, $\zeta = 0{\cdot}02$.

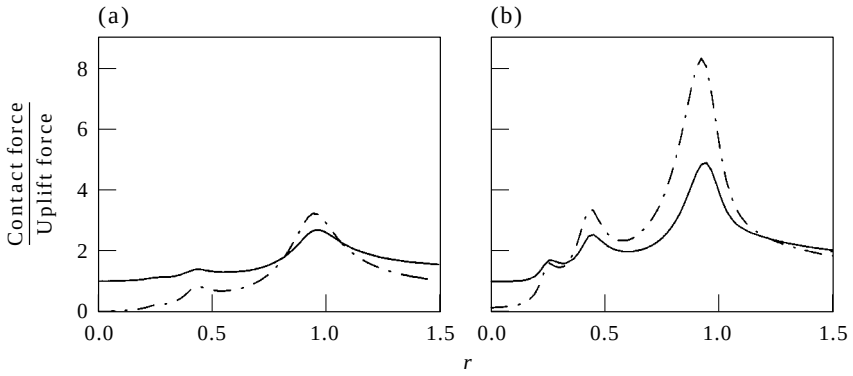

Figure 6. Maximum and peak-to-peak normalised contact forces, $\zeta = 0{\cdot}1$ and $f = 1$: (a) $\alpha = 0{\cdot}3$; (b) $\alpha = 0{\cdot}6$. ——, Maximum contact force; –·–·, peak-to-peak contact force.

The steady-state response of the pantograph–catenary system to the constant uplift force consists of a DC component and some harmonic motion with a dominant component having frequency r. The response is a maximum when r is close to 1/3, 1/2 and 1. By multiplying the displacement $y(t)$ by the instantaneous stiffness $K(t)$ the contact force can be determined.

The peak-to-peak and maximum normalised contact forces are plotted in Figures 6(a) and (b) for $\alpha = 0{\cdot}3$ and $0{\cdot}6$, respectively. For a high-speed railway system $r = 1$ corresponds to approximately 420 km/h and for a mid-speed railway system $r = 1$ corresponds to about 380 km/h. It can be seen that the stiffness variation coefficient α of the catenary in a single span has a significant effect because it is the source of the parametric excitation. As α reduces, so does the variation in contact force. When the peak-to-peak graph exceeds the maximum graph, the minimum contact force will be zero and loss of contact and subsequent current interruption will occur. Thus, the speed corresponding to the first cross-over point of the maximum and peak-to-peak contact force graphs represents upper limits for the operational speeds of trains. For a compound catenary ($\alpha = 0{\cdot}3$) the highest operational speed is governed in the area near $r = 1$ and for a simple catenary ($\alpha = 0{\cdot}6$) in the area near $r = 1/3$. Increasing the stiffness of the catenary or/and decreasing the mass of the pantograph will be beneficial since this will raise the system's nominal natural frequency.

3. DYNAMIC STIFFNESS OF THE OVERHEAD WIRE SYSTEM

Since the catenary in the model discussed above is treated as massless, the effect of the flexural wave propagation in the wire on the pantograph is omitted. If one still wants to take advantage of this model to predict the dynamic behaviour of the pantograph–catenary system, the dynamic stiffness of the catenary should be used instead of the static stiffness. The dynamic stiffness of the catenary is defined as the ratio of the load to the displacement caused by this load. However, this load travels along the catenary with a steady speed, and in this case the displacement of the catenary will vary when the moving speed of the load changes. Therefore, prior to investigating the dynamics of the pantograph–catenary system, the dynamic response of the catenary to a moving load should be studied first.

3.1. SIMPLIFIED MODEL OF THE OVERHEAD WIRE SYSTEM

The first order natural frequency of the overhead system is usually lower than and near to 1 Hz [6] and the corresponding wavelength is equal to twice of the span length. In low frequency vibration modes each catenary of the overhead system moves in phase and the wavelength is much longer than the dropper span. Thus, if the higher frequency vibration is neglected, the overhead system may be regarded as one uniform string with elastic supports. A simplified model of the overhead wire system is shown in Figure 7, which has been studied previously by Manabe [9]. It is an infinite periodically spring-supported string, where T and ρ are the tension and the density of the string respectively, L is the span length, K_S represents the elastic supports of the string and F is a travelling load with a steady speed V. First, some important factors such as T, ρ and K_S in this model should be determined according to the parameters of a real catenary system.

In general T, ρ and K_S may be determined approximately as follows:

$$T = \sum_{i=1}^{n} T_i, \qquad \rho = \sum_{i=1}^{n} \rho_i, \qquad K_S = K_{max} - \frac{2T}{L}, \tag{7a, b, c}$$

where T_i and ρ_i are the tension and the density of the ith catenary in the overhead wire system respectively, K_{max} is the maximum static stiffness in a span. To validate the approximations in equations (7a, b, c) compare the static stiffness and the natural frequencies of the simplified model with those of the original catenary model shown in Figure 2. The results are obtained using the FEM and only three spans have been included for simplicity. Although the boundary conditions at the ends of the first and third spans affect the results, it is very limited. This is because a single span is 50–60 m long and the middle span is less affected by the boundary conditions. Furthermore, the aim of calculation is to validate the simplified model, and both the original model and the simplified model are calculated with the same number of spans. The static stiffness of two types of catenary is shown in Figure 8, and it can be seen that the results of two models are very close to each other. The natural frequencies of the first 12 modes for compound and simple catenaries are listed in Tables 1 and 2, respectively. It can be seen that the low order natural frequencies of the simplified model are generally lower than those of the original model. The reason for this is that the freedom of motion of each catenary in the original model is gradually reduced from the bottom to the top, but in the simplified model there is only one catenary which has as much freedom of motion

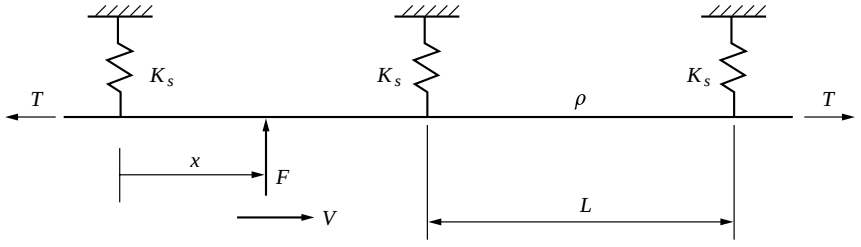

Figure 7. Simplified model of the overhead wire.

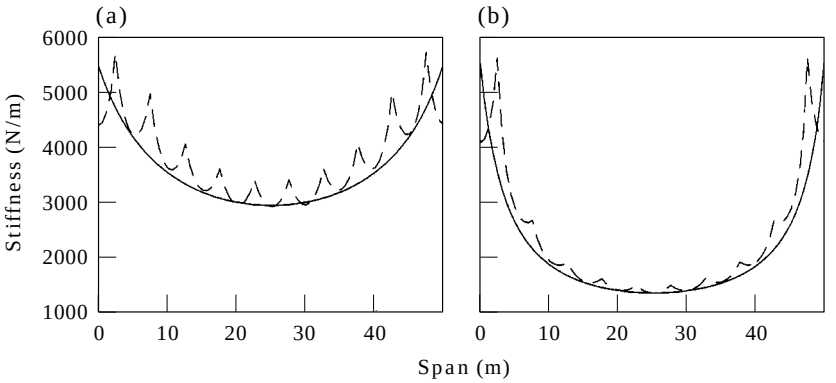

Figure 8. Static stiffness of the catenary: (a) compound catenary; (b) simple catenary. ——, Simplified model; – – –, original model.

as the lowest single catenary in the original model, thus leading to lower natural frequencies.

3.2. RESPONSE OF THE CATENARY TO A MOVING LOAD

Analysis of the dynamic response of an infinite periodic structure to a moving load can be treated in various ways. One approach is by means of the Fourier transform using Floquet's theory and considering only one unit of the periodic structure. Smith and Wormley [14] studied the response of a continuous periodically pin-supported beam to a moving load at constant speed using this

TABLE 1

Natural frequencies of the compound catenary (Hz)

Modes	1	2	3	4	5	6
Simplified model	0·6748	0·9143	1·1148	1·6219	1·9528	2·2289
Original model	0·9356	1·0523	1·1261	1·8505	2·0730	2·2354
Modes	7	8	9	10	11	12
Simplified model	2·6813	3·0349	3·3414	3·7691	4·1300	4·4516
Original model	2·7633	3·0555	3·3087	3·7004	4·0134	4·3166

TABLE 2

Natural frequencies of the simple catenary (Hz)

Modes	1	2	3	4	5	6
Simplified model	0·8787	1·0013	1·0784	1·8031	2·0618	2·1561
Original model	0·9886	1·0370	1·0632	1·9745	2·0712	2·1247
Modes	7	8	9	10	11	12
Simplified model	2·7795	3·0484	3·2322	3·7915	4·0913	4·3062
Original model	2·9554	3·1002	3·1832	3·9298	4·1211	4·2367

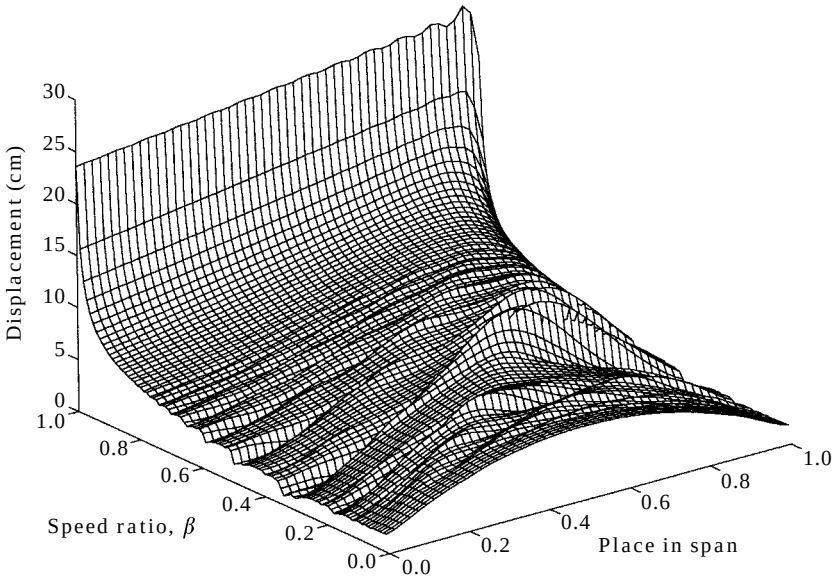

Figure 9. Dynamic response of a simple catenary to a moving load, $\zeta_c = 0{\cdot}02$, $T = 20$ kN, $L = 50$ m, $K_S L/T = 12{\cdot}5$ and $F = 100$ N.

method. The same methodology is used in this paper but for a periodically spring-supported string subjected to a moving load.

The equation of motion and the boundary conditions for the model shown in Figure 7 are

$$\frac{\partial^2 y}{\partial t^2} + \eta \frac{\partial y}{\partial t} - c^2 \frac{\partial^2 y}{\partial x^2} = \frac{F}{\rho} \delta(x - Vt), \tag{8a}$$

$$y(nL^-, t) = y(nL^+, t), \tag{8b}$$

$$K_S y(nL, t) = Ty'(nL^+, t) - Ty'(nL^-, t), \tag{8c}$$

where y' represents the derivative of y with respect to x, n is an integer denoting the nth support, L^- and L^+ denote the left and the right segments of the span at a support point, respectively, η denotes viscous damping and $c = \sqrt{T/\rho}$ is the propagating wave speed in the string.

Introducing the following Fourier transforms:

$$y(x, t) = \frac{F}{2\pi\rho} \int_{-\infty}^{+\infty} Y(x, k)\, \mathrm{e}^{\mathrm{i}k(x - Vt)}\, \mathrm{d}k, \tag{9}$$

$$\delta(x - Vt) = \frac{1}{2\pi} \int_{-\infty}^{+\infty} \mathrm{e}^{\mathrm{i}k(x - Vt)}\, \mathrm{d}k, \tag{10}$$

where $Y(x, k)$ is the transform of $y(x, t)$, $\mathrm{i} = \sqrt{-1}$ and k is the wave number, then

$$\frac{\partial y}{\partial t} = \frac{F}{2\pi\rho} \int_{-\infty}^{+\infty} -\mathrm{i}kVY(x, k)\, \mathrm{e}^{\mathrm{i}k(x - Vt)}\, \mathrm{d}k, \tag{11a}$$

$$\frac{\partial y}{\partial x} = \frac{F}{2\pi\rho}\int_{-\infty}^{+\infty} [Y'(x,k) + \mathrm{i}kY(x,k)]\,\mathrm{e}^{\mathrm{i}k(x-Vt)}\,\mathrm{d}k, \tag{11b}$$

$$\frac{\partial^2 y}{\partial t^2} = \frac{F}{2\pi\rho}\int_{-\infty}^{+\infty} -k^2V^2Y(x,k)\,\mathrm{e}^{\mathrm{i}k(x-Vt)}\,\mathrm{d}k, \tag{11c}$$

$$\frac{\partial^2 y}{\partial x^2} = \frac{F}{2\pi\rho}\int_{-\infty}^{+\infty} [Y''(x,k) + 2\mathrm{i}kY'(x,k) - k^2Y(x,k)]\,\mathrm{e}^{\mathrm{i}k(x-Vt)}\,\mathrm{d}k. \tag{11d}$$

The steady-state response profile of the catenary to a moving load at constant speed is periodic with spacing L, and every span undergoes identical displacements with only a time delay of L/V, that is

$$y(x+nL, t+nL/V) = y(x,t). \tag{12}$$

Thus, using Floquet's principle the transform $Y(x,k)$ is periodic with respect to the spatial co-ordinate x:

$$Y(x+nL,k) = Y(x,k), \tag{13}$$

and therefore

$$Y(nL^+,k) = Y(0,k), \qquad Y(nL^-,k) = Y(L,k), \tag{14a, b}$$

$$Y'(nL^+,k) = Y'(0,k), \qquad Y'(nL^-,k) = Y'(L,k). \tag{14c, d}$$

Substituting equations (9)–(11) and (14) into equation (8) gives the following equations in the wave number domain:

$$Y''(x,k) + 2\mathrm{i}kY'(x,k) + \left[k^2(\beta^2-1) + \mathrm{i}k\beta\frac{\eta}{c}\right]Y(x,k) = -\frac{1}{c^2}, \tag{15a}$$

$$Y(0,k) = Y(L,k) \tag{15b}$$

$$K_S Y(0,k) = TY'(0,k) - TY'(L,k), \tag{15c}$$

where $\beta = V/c$. The solution to equation (15a) is given as follows:

$$Y(x,k) = A\,\mathrm{e}^{-\mathrm{i}(k+s)x} + B\,\mathrm{e}^{-\mathrm{i}(k-s)x} + \frac{1/c^2}{k^2(1-\beta^2) - \mathrm{i}k\beta\dfrac{\eta}{c}}, \tag{16}$$

where $s = \sqrt{k^2\beta^2 + \mathrm{i}k\beta\eta/c}$. If the non-dimensional quantities $\bar{x} = x/L$, $\overline{k} = kL$, $\bar{s} = sL$ and $\eta = 2\pi\zeta_c c/L$ are introduced, then equations (16), (15b) and (15c) can be rewritten as

$$Y(\bar{x},\overline{k}) = A\,\mathrm{e}^{-\mathrm{i}(\overline{k}+\bar{s})\bar{x}} + B\,\mathrm{e}^{-\mathrm{i}(\overline{k}-\bar{s})\bar{x}} + \frac{L^2/c^2}{\overline{k}^2(1-\beta^2) - \mathrm{i}2\pi\zeta_c\overline{k}\beta}, \tag{17a}$$

$$Y(0,\overline{k}) = Y(1,\overline{k}), \tag{17b}$$

$$K_S Y(0,\overline{k}) = TY'(0,\overline{k}) - TY'(1,\overline{k}), \tag{17c}$$

where ζ_c is the damping ratio (when $\zeta_c = 1$, the first order mode of a string with two fixed ends is critically damped). The complex wave amplitudes A and B can be determined using the boundary conditions (17b) and (17c) and thus the final result for Y is given by:

$$Y(\bar{x}, \bar{k}) = \frac{L^2}{c^2(\bar{k}^2 - \bar{s}^2)} \left[1 - \mathrm{i} \frac{\mathrm{e}^{-\mathrm{i}\bar{k}\bar{x}} \sinh \mathrm{i}\bar{s}(1 - \bar{x}) + \mathrm{e}^{\mathrm{i}\bar{k}(1-\bar{x})} \sinh \mathrm{i}\bar{s}\bar{x}}{\dfrac{2T}{K_S L} \bar{s}(\cosh \bar{k} - \cosh \mathrm{i}\bar{s}) + \mathrm{i} \sinh \mathrm{i}\bar{s}} \right], \tag{18}$$

where $\bar{s} = \sqrt{\bar{k}^2\beta^2 + \mathrm{i}2\pi\zeta_c\bar{k}\beta}$.

The response of the catenary to a moving load can be obtained by performing the integration given in equation (9). In order to determine the dynamic stiffness of the catenary, only the response at the point where the moving load is applied need be calculated. This point is at $x = Vt$, so the integration can be simplified to

$$y_{x=Vt} = \frac{F}{2\pi\rho L} \int_{-\infty}^{+\infty} Y(\bar{x}, \bar{k}) \, \mathrm{d}\bar{k}. \tag{19}$$

For performing the integration the following points should be considered:

1. The real part of $\bar{Y}(\bar{x}, \bar{k})$ is even and the imaginary part is odd, so only one side ($\bar{k} \geqslant 0$) needs to be integrated.

2. When the catenary is undamped, $Y(\bar{x}, \bar{k})$ has an infinite number of poles. Therefore, the numerical integration requires some damping to be introduced in the model. If ζ_c is too small, the result of the integration may be unstable even though a tiny step size is employed in performing the integration.

3. Numerical integration requires a finite interval of integration. Considering both accuracy and efficiency the integration is performed over the range of $\bar{k} \leqslant 40$, and a step size of $\Delta\bar{k} = 0{\cdot}02$ is taken.

It can be proved using (18) that if the catenary is undamped, $Y(\bar{x}, \bar{k})$ and hence $y_{x=Vt}$ will be symmetrical with respect to the middle of a span.

Figure 9 shows the dynamic response of a simple catenary to a moving load, where typical parameters have been chosen, for example, $\zeta_c = 0{\cdot}02$, $T = 20$ kN, $L = 50$ m, $K_S L/T = 12{\cdot}5$ and $F = 100$ N. For a compound catenary the value of $K_S L/T$ is much smaller than that of a simple catenary, being about 3·5. The shape of the dynamic response of a compound catenary is similar to that of the simple catenary but much smoother, so the response graph for a compound catenary is not presented here. When the speeds of the moving load are quite low ($\beta < 0{\cdot}1$), the maximum displacement appears approximately in the middle of a span. In the case of $\beta = 0$ the graph shows the static displacement. From about $\beta > 0{\cdot}3$ the peak displacement appears in the downstream half of the span and moves towards the support end with increasing the speed of the moving load. When the speeds of the moving load are close to the propagating wave speed in the wire ($\beta \to 1$), the dynamic displacements increase dramatically, as can be seen in Figure 9. The local maximum displacements appear in the area from $\beta = 0{\cdot}34$ to 0·55.

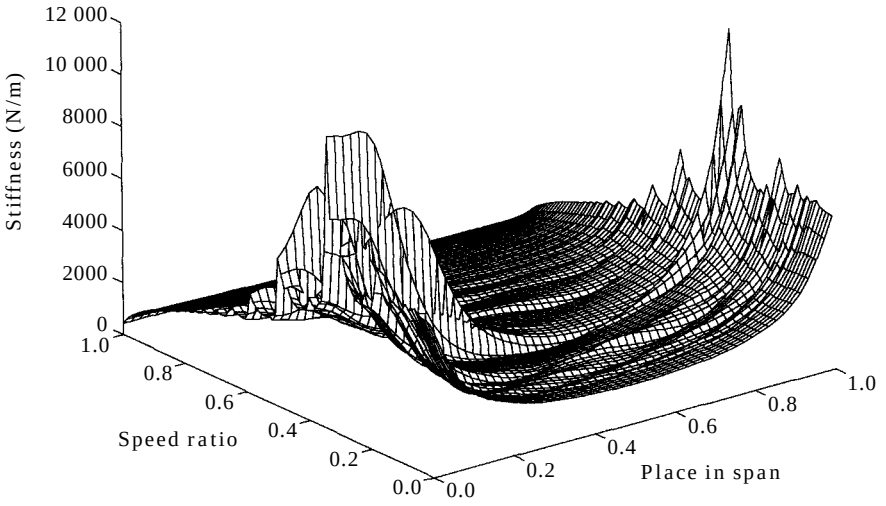

Figure 10. Dynamic stiffness of a simple catenary.

3.3. DYNAMIC STIFFNESS OF THE OVERHEAD WIRE SYSTEM

From the data used in Figure 9 the dynamic stiffness can be obtained by dividing the moving load by the dynamic displacement caused by this load. Figure 10 shows the dynamic stiffness. It can be seen that the dynamic stiffness varies with the speed

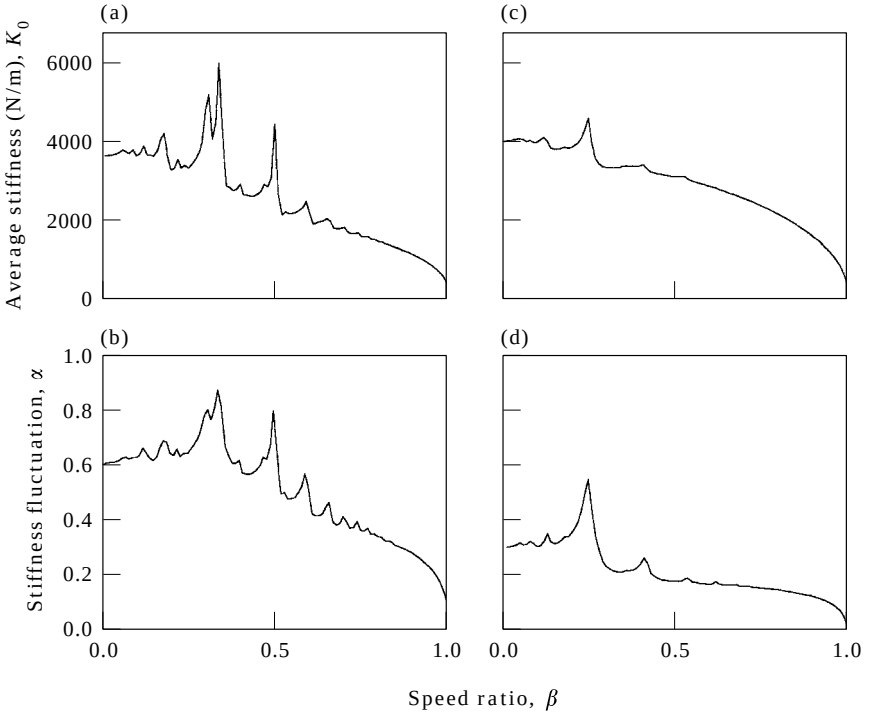

Figure 11. Variation of the dynamic stiffness: (a) and (b) for a simple catenary, where $\zeta_c = 0{\cdot}02$, $T = 20$ kN, $L = 50$ m, $K_S L/T = 12{\cdot}5$; (c) and (d) for a compound catenary, where $\zeta_c = 0{\cdot}02$, $T = 50$ kN, $L = 50$ m, $K_S L/T = 3{\cdot}5$.

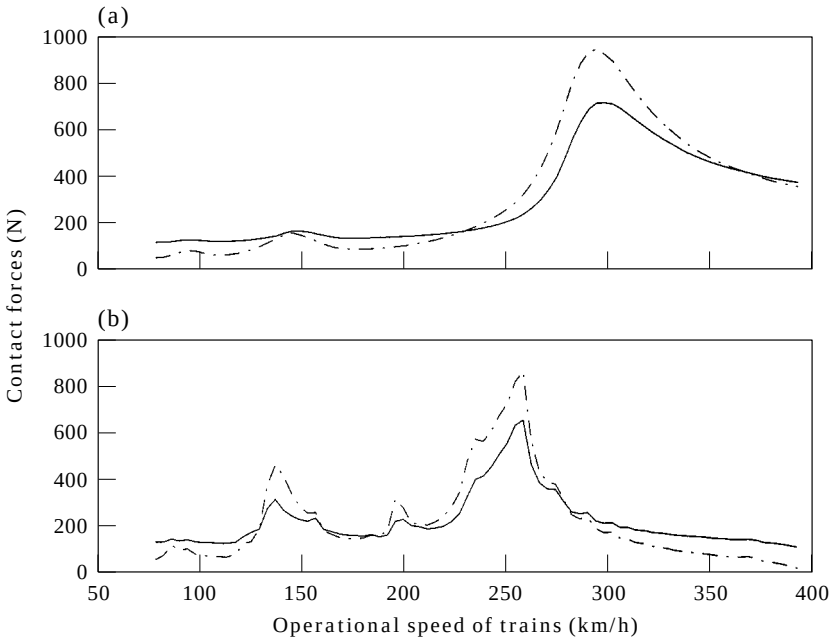

Figure 12. Maximum and peak-to-peak contact forces of a mid-speed railway: (a) using the static stiffness; (b) using the dynamic stiffness. ——, Maximum contact force; –·–·, peak-to-peak contact force.

of the moving load and in general, decreases with increasing the speed from about $\beta = 0{\cdot}3$. There are some dramatic increases of the dynamic stiffness near the support when $\beta = 0{\cdot}3$–$0{\cdot}6$. The effect of the dynamic stiffness variation on the pantograph–catenary system dynamics will be discussed in the next section.

4. DYNAMIC BEHAVIOUR OF THE PANTOGRAPH–CATENARY SYSTEM CONSIDERING THE DYNAMIC STIFFNESS OF THE OVERHEAD WIRE

4.1. VARIATION OF THE AVERAGE STIFFNESS AND THE STIFFNESS FLUCTUATION

Although the simple model discussed in section 2 is still useful, it is evident that for a more accurate model the time-varying static stiffness $K(t)$ should be replaced by the dynamic stiffness. Referring to equation (2) K_0 and α can be replaced by the average dynamic stiffness and the dynamic stiffness variation coefficient, respectively. These are calculated using equation (2) but the dynamic stiffness shown in Figure 10 rather than the static stiffness is now used to determine these values. Figure 11 shows the calculated values of K_0 and α. Figures 11(a) and (b) represent the simple catenary and Figures 11(c) and (d) represent the compound catenary. It can be seen that both the average dynamic stiffness and the dynamic stiffness variation coefficient are roughly constant when the speed ratio $\beta < 0{\cdot}2$. After that there are several sharp peaks at about $\beta = 0{\cdot}32$ and $0{\cdot}5$ for the simple catenary and one sharp peak at about $\beta = 0{\cdot}25$ for the compound catenary and then they both gradually decrease with some small peaks. Therefore, the overhead

wire appears softer and has a larger "static" displacement when train speed increases, and the magnitude of the forcing function decreases.

4.2. THE EFFECT OF CATENARY'S DYNAMIC STIFFNESS VARIATION ON THE PANTOGRAPH–CATENARY SYSTEM DYNAMICS

Since the model described by equation (4) remains valid, the formats of Figures 5 and 6 are still useful in the analysis of the dynamic behaviour of the pantograph–catenary system, but now the dynamic rather than the static stiffness of the catenary has to be used. However, because the dynamic stiffness varies with train speed, it will lead to some differences in the interpretation of the dynamic behaviour of the system by using these figures. Compared with the case of using the static stiffness, the effects of the dynamic stiffness variation on the dynamic behaviour of the pantograph–catenary system may be summarised as follows:

1. The system's nominal natural frequency ω_n is no longer constant. It varies with the train's travelling speed. In general it will decrease with increasing train speed because the average dynamic stiffness of the catenary decreases when the non-dimensional speed of the train increases above about $\beta = 0{\cdot}2$ except some stiffness peak areas. This will have a detrimental effect on the dynamic performance of the pantograph–catenary system because a specific value of r now corresponds to a lower train speed in Figures 5 and 6.

2. The dynamic stiffness variation coefficient α decreases with increasing the speed of the train from $\beta = 0{\cdot}5$ for the simple catenary and $\beta = 0{\cdot}3$ for the compound catenary, and this has a beneficial effect on the system's performance.

3. The damping ratio ζ of the system is also not constant. It rises when train speed increases because the system's nominal natural frequency ω_n decreases with increasing train speed. This will also have a beneficial effect on the system's performance.

4. Regarding the pantograph–catenary system's stability boundaries, Figure 5 is still valid, but the way of using this figure is slightly different. Since the system's nominal natural frequency decreases with increasing train speed, the corresponding speeds to three unstable areas, which occur in regions around $r = 2/3$, 1 and 2, will be lower than when the static stiffness of the catenary is considered. Moreover, it should be noticed that other two factors, α and ζ, which affect the system's stability are now functions of train speed. Although the dynamic stiffness of the catenary becomes softer with increasing train speed, the pantograph–catenary system will still remain stable in the present speed range because α decreases and ζ increases.

5. To analyse the dynamic contact force Figure 6 can still be used, but similar factors to those discussed in point 4 above should be taken into consideration. The maximum responses still appear close to $r = 1/3$, $1/2$ and 1, but the corresponding speeds are now lower. Because α decreases and ζ increases with increasing train speed, the dynamic contact force and its fluctuation gradually reduce at higher speeds, compared to those predicted by the simple model using only the static stiffness of the catenary.

5. NUMERICAL EXAMPLES

The SDOF model discussed above that employs a dynamic stiffness of the catenary is acceptable for the analysis of the basic dynamic behaviour of the pantograph–catenary system. However, the accuracy of the results may be poor because the dynamic stiffness $K(t)$ has the form of equation (2), but in fact it is not quite as simple as this in reality (see Figure 10). In addition the connection between the head and the frame of the pantograph is regarded as rigid in the SDOF model, but in reality there is an elastic suspension between them.

To obtain more accurate results two numerical examples are calculated. One represents a mid-speed railway and the other a high-speed railway. The pantographs of two systems are the same and are represented by the 2DOF model shown in Figure 4(a). The following parameters are employed for the pantograph: $M_1 = 8$ kg, $M_2 = 12$ kg, $K_1 = 10$ kN/m, $C_1 = 120$ Ns/m, $C_2 = 30$ Ns/m, $F_L = 100$ N.

The catenaries of the two systems have different parameters. The parameters for the mid-speed railway system are: $T = 20$ kN, $\rho = 1{\cdot}685$ kg/m, $L = 50$ m, $K_S L/T = 12{\cdot}5$, $\zeta_c = 0{\cdot}02$. The parameters for the high-speed railway system are: $T = 50$ kN, $\rho = 4{\cdot}336$ kg/m, $L = 50$ m, $K_S L/T = 3{\cdot}5$, $\zeta_c = 0{\cdot}02$. The static and dynamic stiffness $K(t)$ of the catenary is represented by a series of discrete values obtained using the procedure discussed in section 3.

The numerical simulation results for the contact force are obtained using the 4th order Runge–Kutta method. Figures 12 and 13 show the contact force in the form of peak-to-peak and maximum values at different operational speeds.

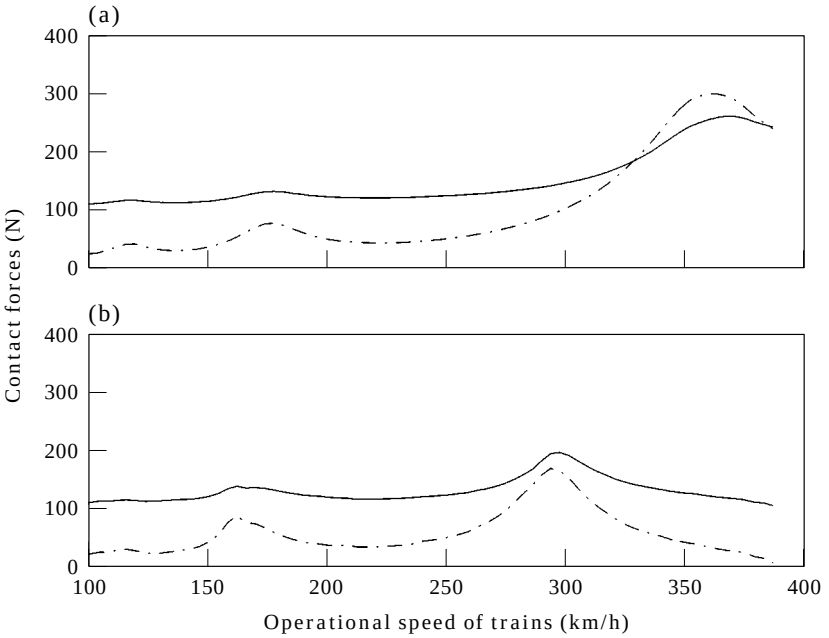

Figure 13. Maximum and peak-to-peak contact forces of a high-speed railway: (a) using the static stiffness; (b) using the dynamic stiffness. ——, Maximum contact force; –·–·, peak-to-peak contact force.

Figure 12 is for the mid-speed railway and Figure 13 for the high-speed railway. Figures 12(a) and 13(a) show the results when the static stiffness of the catenary is used and, Figures 12(b) and 13(b) show the results when the dynamic stiffness of the catenary is used. Compared with the results of the SDOF model, some main points may be summarised as follows.

The graphs in Figures 12 and 13 also have three peak values of the dynamic response approximately corresponding to $r = 1/3$, $1/2$ and 1. This means that the SDOF model can adequately describe the basic dynamic behaviour of the pantograph–catenary system.

There are some other small local peaks of the dynamic response for the mid-speed railway. The reason for this is that there are some peak values at certain train speeds for the dynamic stiffness fluctuation coefficient α which affects the dynamic response significantly. The most noticeable peak is at about 195 km/h which corresponds to speed ratio $\beta = 0{\cdot}5$ where α has a sharp peak value.

The main peak responses of the 2DOF model using the static stiffness of the catenary either for the mid-speed railway or for the high-speed railway appear at lower speeds, compared with the SDOF model (in the case of SDOF model the main peak responses appear at about 380 and 420 km/h for the simple and compound catenaries, respectively). There are two reasons for this. One is that the connection between the head and the frame of the pantograph is elastic in the 2DOF model instead of rigid in the SDOF model. This will lead to a lower natural frequency of the system and hence a lower corresponding speed when $r = 1$. The other reason is that the average stiffness of the catenary in the SDOF model, which is used for calculating system's nominal natural frequency by the equation $\omega_n^2 = K_0/M$, is a simple mean value (see equation (2b)), but in fact the stiffness of the catenary has a much lower value at most places in a span and only rises to its maximum value near the support point (see Figure 8(b)).

When using the dynamic rather than static stiffness of the catenary, the response graphs (shown in Figures 12(b) and 13(b)) are shifted towards a lower speed, compared with those when the static stiffness is used in the model (shown in Figures 12(a) and 13(a)). This characteristic has already been predicted in section 4 (see point 5 in section 4.2) and now is validated in the 2DOF model.

From Figure 13 for the high-speed railway it can be seen that the maximum contact force is always greater than the peak-to-peak contact force when the dynamic stiffness of the catenary is used in the model. This means that the contact force is always positive and thus loss of contact will not occur. The reason for this is that α decreases and ζ increases with increasing train speed. This has a beneficial effect on the system's performance and was discussed for the SDOF model in section 4.

6. CONCLUSION

In this paper the dynamic behaviour of a pantograph–catenary system has been studied. First a periodically excited SDOF model for the pantograph–catenary system was introduced and its basic dynamic behaviour was discussed. To

investigate the effect of the wave propagation in the overhead wire on vibration of the pantograph the dynamic stiffness of the catenary has to be introduced into the SDOF model of the combined pantograph–catenary system. The dynamic stiffness of the catenary was determined by representing it as an infinite periodically spring-supported string.

The results have shown that the dynamic stiffness of a catenary varies with train speed. There are some speeds at which the dynamic stiffness increases dramatically near the support points of the catenary. Except for these speeds, it appears softer and its variation in a span decreases with increasing train speed. This means that the nominal natural frequency of the pantograph–catenary system also varies with train speed and reduces with increasing the speed. It has been shown that this may have a detrimental effect on the performance of the pantograph–catenary system, but because the dynamic stiffness variation decreases with increasing train speed, there may also be some positive effects.

Finally, two numerical examples of a 2DOF model of a pantograph–catenary system have shown that although the SDOF model can give physical insight into the dynamic behaviour of the pantograph–catenary system, it is not as accurate because the average stiffness K_0 in the model is too simple a representation.

REFERENCES

1. G. Poetsch *et al*. 1997 *Vehicle System Dynamics* **28**, 159–195. Pantograph/catenary dynamics and control.
2. T. X. Wu 1996 *Journal of the Chinese Railway Society* **18**(3), 44–49. Analysis and calculation of catenary by FEM.
3. J. R. Ockendon and A. B. Taylor 1971 *Proceedings of the Royal Society of London, Series A* **322**, 447–468. The dynamics of a current collection system for an electric locomotive.
4. T. Vinayagalingam 1983 *ASME Journal of Dynamics Systems, Measurement and Control* **105**, 287–294. Computer evaluation of controlled pantographs for current collection from simple catenary overhead equipment at high speed.
5. T. X. Wu 1996 *Journal of the Chinese Railway Society* **18**(4), 55–61. Study of current collection from catenary–pantograph at high speed by simulation.
6. D. N. Wormley, W. P. Seering, S. D. Eppinger and D. N. O'Connor 1984 *Report No. DOT/OST/P*34-85/023, US Department of Transportation. Dynamic performance characteristics of new configuration pantograph–catenary systems.
7. T. Yagi, A. Stennson and C. Hardell 1996 *Vehicle System Dynamics* **25**, 31–49. Simulation and visualisation of the dynamic behaviour of an overhead power system with contact breaking.
8. T. X. Wu and M. J. Brennan 1998 *Journal of Vehicle System Dynamics* (in press). Basic analytical study of pantograph–catenary system dynamics.
9. K. Manabe 1994 *Quarterly Report of RTRI* **35**, 112–117. Periodical dynamic stabilities of a catenary–pantograph system.
10. L. Frýba 1972 *Vibration of Solids and Structures Under Moving Loads*. Groningen: Noordhoff International Publishing.
11. K. Manabe and Y. Fujii 1989 *Quarterly Report of RTRI* **30**, 175–180. Overhead system resonance with multi-pantographs and countermeasures.
12. A. Nayfeh 1979 *Nonlinear Oscillations*. New York: Wiley.

13. T. X. Wu and M. J. Brennan 1997 *ISVR Technical Memoranum*, No. 819. Analytical study of pantograph–catenary system dynamics.
14. C. C. Smith and D. N. Wormley 1975 *ASME Journal of Dynamics Systems, Measurement, and Control* **97**, 21–29. Response of continuous periodically supported guideway beams to travelling vehicle loads.